Available online at www.sciencedirect.com
ScienceDirect
International Journal of Heat and Mass Transfer 51 (2008) 4958–4965
International Journal of HEAT and MASS TRANSFER
www.elsevier.com/locate/ijhmt

Mechanisms of thermal nanofluids on enhanced critical heat flux (CHF)

Dongsheng Wen *

School of Engineering and Materials Science, Queen Mary University of London, London E1 4NS, UK

Received 9 January 2007
Available online 20 May 2008

Abstract

Research on thermal nanofluids has progressed rapidly since their enhanced thermal conductivities were identified about a decade ago. Thermal nanofluids have been observed to increase the critical heat flux (CHF) remarkably under pool-boiling conditions, which could not be explained by conventional theories developed for pure fluids. This paper proposes an alternative mechanism, the long-range structural disjoining pressure arising from the confinement of nanoparticles in a meniscus, and investigates its role under high heat flux conditions. The structural disjoining pressure is incorporated into a four-zoned dry patch model and an analytical model is established to calculate the equilibrium meniscus shape in the presence of nanoparticles. The results show that the structural disjoining pressure can significantly increase the wettability of the fluids and inhibit the dry patch development. Other possible mechanisms on the enhanced CHF are discussed and future studies to resolve remaining issues are recommended.

Keywords: Nanofluids; Nanoparticles; Structural disjoining pressure; Boiling; Critical heat flux; Dryout

1. Introduction

Recent advances in nanotechnology have promoted a rapid development in *nanofluids*, liquid suspensions of nanoparticulate solids including particles, nanofibers and nanotubes. Such materials were first brought into attention approximately a decade ago when their enhanced thermal conductivities were observed [4]. However to differentiate it from classical colloid dispersions, a more suitable name *thermal nanofluids* has been coined [23]. While the original idea of using thermal nanofluids was to enhance thermal conductivities of some typical heat transfer fluids including water, mineral oil and ethylene glycol, the inclusion of nanoparticles has been found more profound than the mean thermal conductivity effect. Many contradictory results have been reported especially under pool-boiling conditions [5,24,1], this however does not prevent them being promising heat transfer fluids in the future for applications in power plants, automobile industry, heating ventilating and air conditioning (HVAC) and a wide range of other energy related fields.

Quite a few studies have shown that very dilute thermal nanofluids could significantly increase the critical heat flux (CHF) under pool boiling conditions [27,19,14]. You et al. [27] investigated aluminum–water nanofluids on a 10 by 10 mm^2 heater under sub-atmospheric pressure conditions. Over 200% enhancement of CHF was observed at a nanoparticle volume concentration of 0.001%. It was observed in the experiments that thermal nanofluids increased bubble size and decreased bubble departure frequency, which could contribute partly to the observed CHF enhancement. Similar high CHF enhancement was also observed by Vassallo et al. [19] and Milanova and Kumar [14] for pool boiling of silica–water nanofluids on horizontal heating wires under atmospheric pressure conditions. The particle size ranged from 10 to 3000 nm in these experiments. The results showed that ~200% enhancement in CHF was achieved at a volume concentration of 0.5% for 15 nm silica nanofluids [19], and ~300% enhancement at a volume concentration of 0.2% for 20 nm particles [14]. The influence of nanoparticle size and concentration on CHF, however, was not clear. Layers of silica coating (0.025–0.05 mm) were

* Tel.: +44 20 78823232; fax: +44 20 89831007.
E-mail address: d.wen@qmul.ac.uk

0017-9310/$ - see front matter © 2008 Elsevier Ltd. All rights reserved.
doi:10.1016/j.ijheatmasstransfer.2008.01.034

Nomenclature

A	Hamakar constant
b	radius of curvature (m)
C	integration constant in Eq. (2)
d	diameter (m)
g	gravitational acceleration (m/s^2)
h	film thickness (m)
h_{lv}	latent heat (J/kg)
k	Boltzmann constant
n_0	bulk concentration (%)
P	bulk osmotic pressure (Pa)
p	pressure (Pa)
p_d	disjoining pressure (Pa)
p_e	electrostatic pressure (Pa)
q	heat flux (kW/m^2)
T	temperature (°C)
s	arc length (m)
W	film energy (J)
x	horizontal coordinate
y	vertical coordinate

Greek symbols

σ	interfacial tension (N/m)
Π	structural disjoining pressure (Pa)
Π_0	amplitude coefficient in Eq. (6)
Π_1	amplitude coefficient in Eq. (6)
θ	running angle (°)
ϕ_2	phase of oscillations (°)
Φ	volume concentration (%)
φ	surface potential (V)
κ	Debye length (m)
ω	frequency of oscillation (Hz)
γ	defined as $\tanh(e\varphi/4kT)$
δ	decay parameter in Eq. (6)

Subscripts

l	liquid
v	vapor
∞	infinite

observed on heating wires at the end of the experiments by Vassallo et al. [19], which were suggested as an enhanced surface roughness effect that contributed to the enhancement of CHF. Different ionic and electrolyte concentrations were suggested by Milanova and Kumar [14] as possible reasons for their observed enhancement.

On the other hand, modest or very low increases in CHF have also been reported. A maximum increase of ~50% in CHF was observed by Bang and Chang [1] for 1% alumina–water nanofluids on a horizontal plate. Further increase of nanoparticle concentrations resulted in a reduced CHF enhancement. A similar trend was obtained by Kim et al. [10] for aqueous based titania and alumina nanofluids on heating wires under atmospheric pressure conditions. In their experiments, the maximum CHF enhancement of ~100% was observed at a volume concentration 0.1% for titania nanofluids. Again it was suggested that CHF enhancement was mainly caused by a layer of nanoparticle coating on the heating surface.

A complete comparison of CHF enhancement data is illustrated in Fig. 1. Note that a logarithmic coordinate is used for the x-axis in order to include all the data and a unified volume concentration is used for easy comparison. All these experiments clearly show that CHF can be increased by thermal nanofluids; however there exists a wide scattering of data. The enhancement can vary from 20% to 300% at similar nanoparticle concentrations. The influence of nanoparticle property, concentration and size are far from conclusive. Such observations could not be explained by the modification of fluids properties and surface effect only. As suggested by You et al. [27], there might be some hidden factors that need to be identified.

The mechanisms of CHF of pure fluids have been developed for a few decades, however little mechanistic analysis of boiling heat transfer with thermal nanofluids has been conducted. Thermal nanofluids may behave more as pure fluids than conventional suspensions of micrometer or millimeter particles, but they are two-phase in nature and should possess some features of conventional suspensions. The interaction of nanoparticles with the heating surface and subsequent modification of surface properties could change boiling behavior significantly. More interestingly, latest development in colloidal science reveals that a long-range structural disjoining pressure will be formed at confined spaces [20] for nanoparticle suspensions. Such a structural disjoining pressure could become important at meniscus of dry patches under high heat flux conditions that could subsequently affect the occurrence of CHF, which will be the main focus of this work.

2. CHF mechanisms of pure liquid

The CHF mechanism of pure fluids has been traditionally described by the hydrodynamic model [11,31,12]. Such a model considers the interfacial stability of vapor outflows. CHF occurs when the velocities of vapor jets from the heating surface reach a critical value where vapor jets become Kelvin–Helmholtz unstable. It is generally assumed that the jet diameter is half of the jet spacing that is bounded by the critical and the most dangerous Taylor wavelengths. Such a concept can be described as a 'far-field' model where the mechanism is controlled by the hydrodynamic stability far away from the heating surface. The validity of the hydrodynamic model has been questioned by a number of researchers since 1980's [7,6,29]. A number of studies have

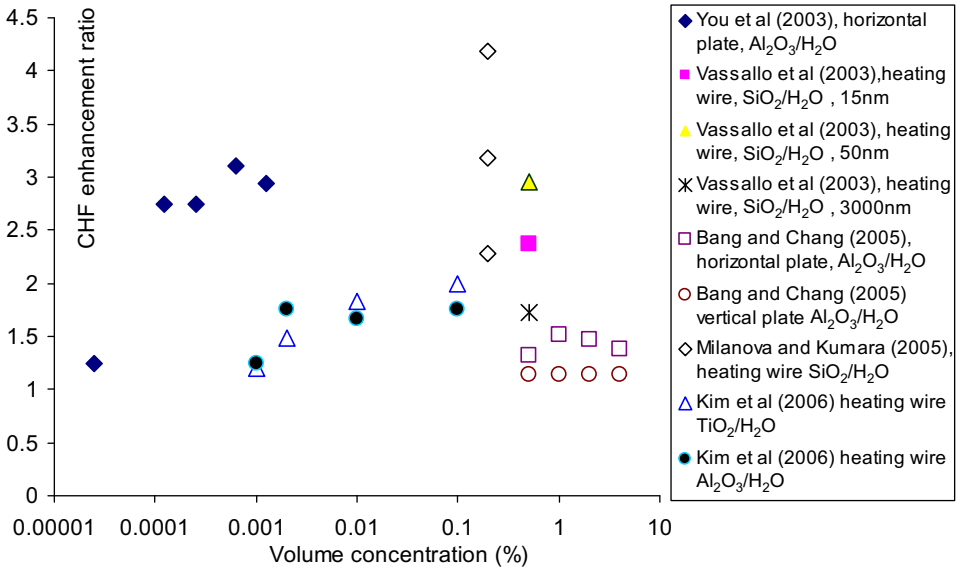

Fig. 1. Literature data on CHF enhancement ratio using thermal nanofluids.

found that the CHF is likely to be controlled by some 'near-field' factors: parameters related to the heating surface involving interactions between vapor, liquid and solid surfaces. Based on the observation of the presence of large vapor mushroom-type bubbles rather than vapor jets on the heating surface, Haramura and Katto [7] suggested that the hydrodynamic instability occurred at the interface of vapor stems supporting the mushroom-type bubble. CHF was proposed to occur when the liquid film trapped between the base of the mushroom-type bubble and the wall dried out prior to the departure of the mushroom-type bubble (hovering period). Such a dryout model was later developed by Haa and No [28] and Zhao et al. [30]. One of the important 'near-field' factors, the effect of surface wettability on the CHF was observed by a few scholars [6,13], who demonstrated that CHF decreased with increasing contact angles. In parallel to the concept development, the dryout phenomena were visualized through a high-speed, high-resolution infrared thermometer by Theofanous et al. [29]. The observations indicated that CHF was controlled by the micro-hydrodynamics and rupture of an extended liquid microlayer. It was the rupture of the liquid microlayer under certain conditions and subsequent dry patch spreading that caused the CHF [29]. Further evidence of similar scenario was provided recently by Bang et al. [2]. The understanding of the CHF has therefore been shifted from a 'far-field' theory, the hydrodynamic instability of vapor jet, to a 'near-field' theory, the dynamics of meniscus and dryout of microlayers.

3. CHF mechanisms of thermal nanofluids

3.1. Structural disjoining pressure and CHF

3.1.1. The structural disjoining pressure

From the viewpoint of the 'near-field' theory, the CHF is caused by the creation and spreading of dry patches (dryout). As the dynamics of dry patches are controlled by the wall temperature, which is largely affected by the wetting capability of liquid, the understanding of thermal nanofluids on the CHF needs to consider the influence of nanoparticles on the wetting property. Although diluted nanofluids were mostly used by researchers, nanoparticles at confined spaces, i.e microlayers underneath growing bubbles, are much concentrated according to the colloidal science. Besides the effects of evaporation, vapor recoil, capillary force and conventional disjoining pressure from the classical Derjaguin–Landau–Verwey and Overbeek (DLVO) theory, *a long-range structural disjoining pressure* normal to the wall could be arising in a microlayer due to the presence of nanoparticles [20]. Different to the conventional disjoining pressure, which is a result of the London-Van der Waals force that is short-range in nature, it has been demonstrated that the structural disjoining force is generated from the ordering of nanoparticles in a confined wedge (structuring) and the influence can be extended to a film depth of a few nanoparticle diameters (long-range) [20]. The origin of the structural disjoining pressure is due to the confinement of particles in a thin film region as opposed to their greater freedom of location in the bulk liquid. When the film thickness is large enough to accommodate more than one layer of particles, the particles tend to arrange themselves in ordered layers. The layering arrangement of the particles gives rise to an excess pressure in the film, the structural disjoining pressure, which has an oscillatory decay profile with the film thickness. A result of such a structure force is that nano-dispersions could exhibit improved spreading/wetting capabilities at a confined space. Such forces have been observed to reduce the macroscopic contact angle of a liquid droplet [18], stabilize liquid films [16] and lift an oil droplet from a wall in an aqueous solution [20,3]. In all these studies, the modeling of interfacial shapes of

liquid films and droplets were only focused on the hydrodynamics involving no heat transfer.

Similar enhanced spreading capability due to nanoparticles could be expected at solid–liquid–vapor contact line regime (microlayer), which could increase the rewetting ability of the fluids and inhibit dry patch growth to increase the CHF. Such an inhibition effect might have already been reflected in the pool boiling experiments with thermal nanofluids that up to 3 times increase in CHF could be achieved [27,19,14]. The concept of structural disjoining pressure on the microlayer dynamics was proposed by Wen and Ding [24] and Wen et al. [25] to explain possible influences of thermal nanofluids on the nucleate boiling heat transfer. Recently a similar concept was proposed by Sefiane [15] on possible influences on CHF but no modeling work has been reported so far. In order to quantitatively reveal the roles of structural disjoining pressure, a simple analytical model will be developed in this work to calculate the interfacial shape of a dry patch in the presence of different concentrations of thermal nanofluids under CHF conditions. The interface will be modeled under the actions of structural disjoining pressure, capillary force, hydrostatic force and evaporation effect. Due to the complexity involved, the paper is not intended to build a complete model for thermal nanofluids on the CHF, but to reveal possible influences and provide an explanation/mechanism on the increased CHF by incorporating theoretically the influence of the structural disjoining pressure.

3.1.2. The dry patch model

A simplified dry patch model is established to identify possible influences of the structural disjoining pressure on the critical heat flux as illustrated in Fig. 2. The dry patch is assumed to exist underneath an evaporating vapor bubble that supplied by a liquid meniscus. This resembles the near-field controlled CHF model. Compared with the three-zoned model of pure liquid [22], thermal nanofluids include four zones. Zone I is the dry patch regime where no evaporation occurs; it could enlarge or diminish in size depending on the forces acting in the Zone II and Zone III. Zone II is the conventional microlayer regime where the wetting and dynamics of the interface is determined by the effects of evaporation, vapor recoil, capillary force and conventional disjoining pressure derived from the DLVO theory [9]. The conventional disjoining pressure can be generally modeled by a Hamaker constant, A, as $p_d = A/h^n$ that decays rapidly with film thickness, h, and becomes negligible at a film thickness of a few nanometers. Due to its short-range nature, the conventional disjoining pressure becomes negligible in the zone III. Zone III is an extended microlayer that includes a regime of liquid film thickness between one and a few nanoparticle diameters where the structural disjoining pressure comes into play. In Zone III, the conventional disjoining pressure is replaced by the structural disjoining pressure due to the ordering of nanoparticles in the microlayer. The wetting and dynamics of the meniscus in zone III is decided by the effects of evaporation, vapor recoil, capillary force and structural disjoining pressure. Zone IV is the bulk regime and the interface can be described by an extended Young–Laplace equation.

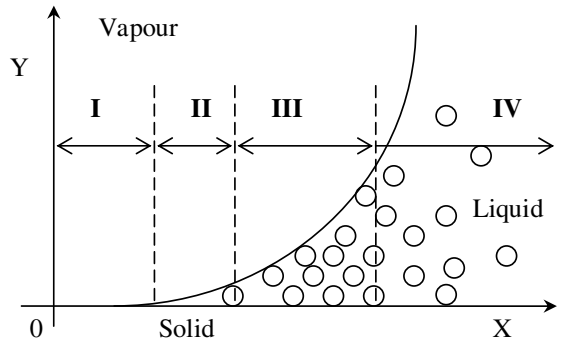

Fig. 2. Four-zoned microlayer model of thermal nanofluids.

The dry patch dynamics are mainly decided by the complicated forces acting in zone II and zone III. The evaporative force tends to enlarge the dry patch area while competing with the conventional disjoining force at a film thickness below a nanoparticle diameter, and the structural disjoining pressure at a film thickness beyond one nanoparticle diameter. Since the structural disjoining pressure can not be extended into zone II, the forces within the zone II will be the same irrespective of the presence of nanoparticles. Consequently the only difference between thermal nanofluids and pure liquids lies in zone III, as modeled below.

3.1.3. The structural disjoining pressure and interfacial shape model

As the paper is not intended to build a complete model of the dry patch and the CHF, but to reveal the possible influence of the structural disjoining pressure, the four-zoned model can be greatly simplified. The forces in zone II will be assumed to be the same for both pure liquids and thermal nanofluids. The role of the structural disjoining pressure will be revealed by calculating interfacial shapes for a pure fluid and different concentrations of thermal nanofluids, as described below.

The shape of the meniscus close to the triple line, where the film thickness measured from the solid surface (h) is of the order of a nanoparticle's diameter. The force balance under a uniform heat flux boundary condition can be written as

$$p_l - p_v = -\frac{\sigma(\mathrm{d}^2h/\mathrm{d}x^2)}{[1+(\mathrm{d}h/\mathrm{d}x)^2]^{3/2}} - \Pi(h) + \Delta\rho g h + \frac{q^2}{2\rho_v h_{lv}^2} \quad (1)$$

where p is the pressure, σ is the interfacial tension, Π is the structural disjoining pressure, $\Delta\rho$ is the density difference between liquid and vapor, $\Delta\rho = \rho_l - \rho_v$, g is the gravitational acceleration, q is the heat flux, h_{lv} is the latent heat, x is the horizontal coordinate, the subscripts l and v refer to the liquid and vapor phase respectively. The first term of

the right hand side in Eq. (1) represents the capillary contribution to the pressure difference, the second term is the structural disjoining pressure, the third term is the gravitational contribution and the last term is due to the heating effect.

Multiplying Eq. (1) by an interfacial slope $\mathrm{d}h/\mathrm{d}x$ and integrating with respect to x gives

$$\frac{\mathrm{d}h}{\mathrm{d}x} = \left[\left(\frac{\sigma}{C - A(h)}\right)^2 - 1\right]^{1/2} \tag{2}$$

Eq. (2) describes the equilibrium meniscus profile under actions of the hydrostatic, capillary, heat flux and structural disjoining pressure, where C is the constant of integration and can be specified by applying Eq. (2) to the Laplace equation, Eq. (3), at $h = h_\infty$

$$\sigma\frac{\mathrm{d}\theta}{\mathrm{d}s} = \frac{\sigma}{b} + y\Delta\rho g \tag{3}$$

where b is the radius of curvature of the dry patch at the apex. Eq. (3) can be solved subject to the boundary conditions on the running angle, θ, arc length, s, horizontal distance from apex, x, and vertical distance from apex, y.

$A(h)$ in Eq. (2) is described by

$$A(h) = \left[(p_l - p_v) - \frac{q^2}{2\rho_v h_{lv}^2}\right](h_\infty - h) + W(h) - \frac{\Delta\rho g}{2}(h_\infty^2 - h^2) \tag{4}$$

where h_∞ is the height of the meniscus far from the wedge, i.e., towards the bulk. This typically corresponds to a film thickness ~5 particle diameters, at which the structural disjoining pressure (Π) contribution is negligible. $W(h)$ is the film energy term that is the integration of the structural disjoining pressure,

$$W(h) = \int_h^\infty \prod(h')\mathrm{d}h' \tag{5}$$

The structural disjoining pressure in a thin liquid film is the excess pressure in the film relative to that in the bulk solution due to the re-arrangement of particles (structuring) in the thin film. This term is dependent upon the nature of the particle ordering that can be described by a radial distribution function. A successful analytical expression for the structural disjoining pressure was given by Trokhymchuk et al. [17] based on a solution of the Ornstein–Zernike equation, as below.

$$\prod(h) = \prod_0 \cos(\omega h + \phi_2)\mathrm{e}^{-\kappa h} + \prod_1 \mathrm{e}^{-\delta(h-d)} \quad \text{for } h \geqslant d \tag{6a}$$

$$\prod(h) = -P \quad \text{for } 0 < h < d \tag{6b}$$

where d is the nanoparticle diameter, κ is the Debye length, ω is the frequency of the oscillation, δ is the short-range decay parameter, ϕ_2 is the phase of oscillations and Π_0, Π_1 are the amplitude coefficients. Such parameters can be fitted as cubic polynomials in terms of particle volume fraction, ϕ. In Eq. (6b), P refers to the bulk osmotic pressure from the nanoparticles. The film energy, Eq. (5), can then be integrated from Eq. (6).

3.1.4. Modeling results

Similar methods as Trokhymchuk et al. [17] were adapted in this work to find solutions of the structural disjoining pressure, Eq. (6), and film energy, Eq. (5), whose values are taken into Eq. (2) to calculate the interfacial shape. In order to understand the structural disjoining pressure, examples of its profile under different nanoparticle concentrations, its comparison with classical DLVO forces and its influence on the interfacial shape of the dry patch are presented below.

Fig. 3 shows the dimensionless structural disjoining pressure, defined as the ratio of structural disjoining force over the thermal perturbation energy, kT, where k is the Boltzmann constant, under different particle concentrations. Due to the layering of nanoparticles in different radial direction, the structural force displays an oscillatory characteristic that decays along the radial direction. The amplitude and frequency of the oscillation force increase with increasing particle concentrations. Depending on the particle concentration, the influence of the structural force can last to a film thickness ~5 nanoparticle diameters.

Fig. 4 compares the structural disjoining forces with the Van der Waals disjoining force and the electrostatic force. A particle diameter of 20 nm at a volume fraction of 0.25 is assumed for the structural disjoining pressure. To calculate the DLVO forces, the retarded form of the conventional disjoining pressure of an aqueous liquid film (3) and two dissimilar bulk phases, vapor (1) and heating surface (2) is expressed in a Hamaker form

$$P_\mathrm{d}(h) = A_{132}/6\pi h^3 \tag{7}$$

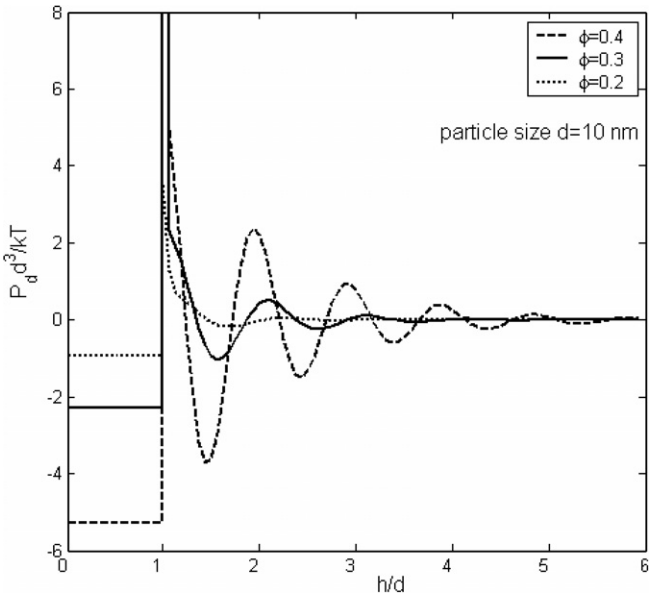

Fig. 3. Dimensionless structural disjoining pressures under different particle concentrations.

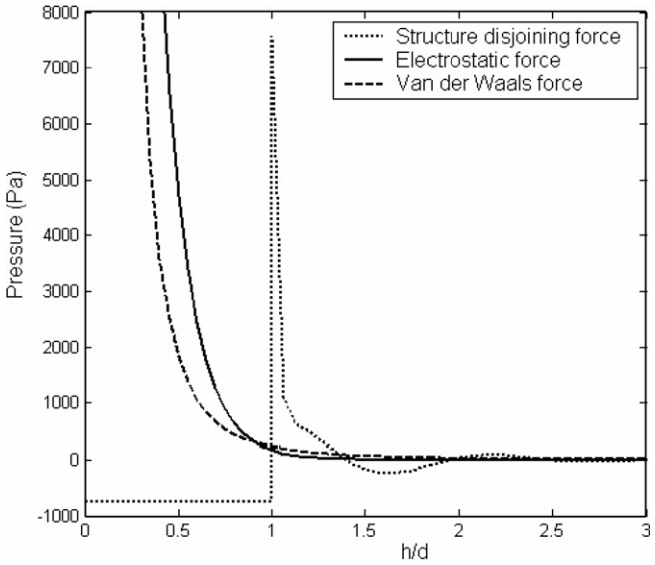

Fig. 4. Comparison of structural disjoining pressure with DLVO forces.

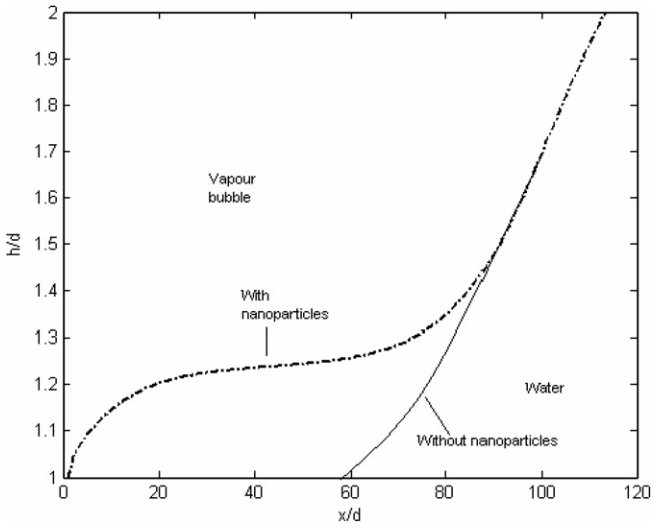

Fig. 5. Interfacial shapes with and without nanoparticles.

where A is the Hamaker constant. For boiling experiments, the heating materials generally are copper, stainless steel and other metals. A Hamaker constant value of 3.45×10^{-20} J is estimated for the calculation. The electrostatic force, P_e, is calculated from Israelachvili [9]

$$P_e(h) = 64kTn_0\gamma^2 e^{-\kappa h} \quad (8)$$

where n_0 is the bulk concentration of a 1:1 electrolyte (taken to be 0.01 M), κ is the Debye length that estimated to be 3 nm, and γ is defined as $\tanh(e\varphi/4kT)$ where φ is the surface potential, which is assumed constant and equal to 30 mV for this calculation.

It can be clearly seen from Fig. 4 that the van der Waals disjoining force and electrostatic force decay rapidly with the film thickness and become negligible at a film thickness less than 1 nanoparticle diameter. The structural disjoining pressure, however, extends to a film thickness of a few nanoparticle diameters. It has a long-range nature and the magnitude is much larger at long distances of separation than the van der Waals and the electrostatic components. This is why the structural disjoining pressure plays a role in determining the meniscus profile.

Fig. 5 compares the steady-state meniscus shape of nanofluids with that of pure water. In the calculation, nanoparticles are assumed spherical with diameter of 20 nm and concentration of 25%; and a heat flux of 1 MW/m^2 and a bulk vapor diameter at of 1 mm are used. For the pure water case where the interface is controlled by the capillary force, gravitational force and heating effect, the liquid–vapor interface meets the heating surface at a radial position of $x/d \sim 60$, which suggests a dry patch diameter of approximately 2.4 μm underneath the vapor. With the introduction of nanoparticles and the structural disjoining pressure, the liquid–vapor interface is pushed toward the vapor center and the triple line is shifted to a radial position of $x/d \sim 2$. This significantly reduces the dry patch diameter to ~80 nm. The dry patch area that exists under pure water conditions has been replaced by a thin layer of liquid at a thickness of ~4 nm. The convex and concave interface shape is correspondent to the structural disjoining pressure profile as shown in Fig. 4, which suggests that the structural disjoining pressure plays a dominant role in determining the interface shape. It is also noted that the interfacial shapes under these two cases overlap at a radial distance $x/d \sim 90$ as the influence of the structural disjoining pressure becomes negligible. The reduction of dry patch area and increased portion of liquid under the vapor can be thought as an increased wettability effect, although its influence should be more profound than the wettability effect only. The presence of nanoparticles in microlayer could increase the microlayer evaporation; enhance the effective thermal conductivity of the liquid layer, as well as inducing a convective effect as particles moving towards the dry patch. Compared with pure fluids, thermal nanofluids have effectively reduced the dried area under similar heating and geometrical conditions. The structural disjoining pressure could therefore delay the occurrence of the CHF. This might have been evidenced by the experimental results where more than 3 times increase in CHF were obtained for thermal nanofluids [27,19].

3.2. Other influence of nanoparticles on the CHF

Besides the structural disjoining pressure effect, the presences of nanoparticles may modify both the liquid properties such as thermal conductivity and viscosity, and the surface properties of the heating wall including cavity size and angle distribution. The modification of liquid properties is marginal when compared with the data scattering in Fig. 1, however the modification of heating surface due to the interaction of nanoparticles with the heating surface should become important under high heat flux condi-

tions, which has been suggested by a number of researchers as possible mechanisms for the observed CHF enhancement [19,10]. Such effects can be classified as the roughness/porous effect, improved wettability effect or modified nucleate sites effect. The porous effect could explain some experimental observations from unstable nanofluids where the instability of nanofluids formed layers of nanoparticles coating on the heating surface [10]. However for stable nanofluids or experiments performed at low heating surface temperature, i.e typical superheat as CHF occurs is ~50 K [27,1], it is difficult to form coating layers. There should have other mechanisms responsible for the observed high CHF values, i.e. the structural disjoining pressure. It is apparent that the modification of heating surface alone could not be the only reason for the observed CHF enhancement. However it is a very important factor as boiling heat transfer is very sensitive to the heating surface. Detailed inspection on the change of heater surface characteristics including wettability, surface roughness, and capillary wicking structure will be very useful in understanding the mechanisms. This however requires further investigation.

It should be of note as well that the nanofluids content could significantly affect the CHF. As dispersants and/or surfactants are often used to stabilize nanoparticle suspensions, they alone could modify the surface tension and wettability of fluids, and influence boiling heat transfer significantly [21,26,8]. However, most published studies on CHF of nanofluids did not clearly specify if surfactants or dispersants were used, which makes the comparison of different experiments difficult. These might be also one of the reasons responsible for the wide data scattering as shown in Fig. 1.

4. Remaining and future work

The present study proposed possible influences of the structural disjoining pressure at the meniscus on the CHF and constructed a simplified dry patch model to illustrate its role in inhibiting the dry patch development. However there are still a number of unsolved issues, especially regarding the transient behavior and the concentration effect.

A steady-state model was employed in this work; a question of interest is that will this structural disjoining pressure still be effective during the transient bubble growth and departure process? Ordered nanoparticle layers have to be formed for the structural disjoining pressure to take place, which will take some time. For boiling under high heat fluxes where mushroom-type large vapor bubbles are presented, the hovering time is much longer than those of individual bubbles under the nucleate boiling regime. However how significant the structural disjoining pressure could be is still unclear. A steady-state model could be only valid if the life time of dry patches is much longer than that of forming ordered nanoparticle layers. Comparison of the time scale shows that the influence of thermal nanofluids on CHF should be more important than that of nucleate boiling regime. This might have been reflected from published experiments where significant increase in CHF is generally observed while the influence of nanofluids on the nucleate boiling regime is small [5,24,1].

Another question to concern is the concentration effect. Low concentrations of thermal nanofluids are usually formulated that could have remarkable influence on CHF. As shown in Fig. 3, however the structural disjoining force only becomes significant at relative high nanoparticle concentrations, i.e. over 20%. Although it has been known that nanoparticles tend to accumulate at confined spaces, quantitative investigation is still needed. Local observation of nanoparticle concentration distribution around a growing bubble will be very useful.

Both experimental and theoretical studies are highly required in order to identify the mechanisms of thermal nanofluids on CHF, and to promote the application of these advanced heat transfer fluids. Future experiments should focus on stable thermal nanofluids with controlled surfactant/dispersant content and on identification of the interaction of nanoparticles with heating surface, especially the modified surface effect. Both transient and concentration effect on the structural disjoining pressure should be developed in future dry patch models, and compared with well-designed experiments. The influence of particle size, shape and distribution on structural disjoining pressure and subsequent CHF occurrence needs to be further identified in order to provide a reasonable explanation on the data scattering shown in Fig. 1.

5. Conclusion

This paper reviewed experiments and possible mechanisms of thermal nanofluids on enhanced critical heat flux (CHF) and identified the important role of the structural disjoining pressure at the meniscus of dry patches. The structural disjoining pressure were calculated and compared with classical DLVO forces, and incorporated into a steady-state dry patch model. The calculated equilibrium interfacial profile showed that the triple line could be significantly displaced towards the vapor phase in the presence of nanoparticles. The result demonstrated that the structural disjoining pressure could increase the wettability and inhibit the dry patch development. Discussion on other mechanisms suggests that beside the structural disjoining pressure effect, possible modification of the heating surface and the surfactant effect are the other potential reasons for the CHF enhancement by thermal nanofluids.

Acknowledgement

The author would like to extend his thanks to EPSRC for financial support under the Grant: EP/E065449/1.

References

[1] I.C. Bang, S.H. Chang, Boiling heat transfer performance and phenomena of Al_2O_3–water nanofluids from a plain surface in a pool, Int. J. Heat Mass Transfer 48 (2005) 2407–2419.

[2] I.C. Bang, S.H. Chang, W.P. Baek, Direct observation of a liquid film under a vapor environment in a pool boiling using a nanofluid, Appl. Phys. Lett. 86 (2005) 134107.

[3] A. Chengara, A.D. Nikolov, D.T. Wasan, Spreading of nanofluids driven by the structural disjoining pressure gradient, J. Colloid Interf. Sci. 280 (2004) 192–201.

[4] S.U.S. Choi, Enhancing thermal conductivity of fluids with nanoparticles, in: Proceedings of the 1995 ASME International Mechanical Engineering Congress and Exposition, San Francisco, CA, USA, 1995.

[5] S.K. Das, N. Putra, W. Roetzel, Pool-boiling characteristics of nanofluids, Int. J. Heat Mass Transfer 46 (2003) 851–862.

[6] V.K. Dhir, S.P. Liaw, Framework for a unified model for nucleate and transition pool-boiling, ASME J. Heat Transfer 111 (1989) 739–746.

[7] Y. Haramura, Y. Katto, A new hydraulic model for critical heat flux, applicable widely to both pool and forced convection boiling on submerged bodies in saturated liquids, Int. J. Heat Mass Transfer 26 (1983) 389–399.

[8] G. Hetsroni, M. Gurevich, A. Mosyak, R. Rozenblit, Z. Segal, Boiling enhancement with environmentally acceptable surfactants, Int. J. Heat Fluid Flow 25 (2004) 841–848.

[9] J.N. Israelachvili, Intermolecular and Surface, Forces, Academic Press, San Diego,CA, 1992.

[10] H. Kim, J. Kim, M.H. Kim, Effect of nanoparticles on CHF enhancement in pool-boiling of nanofluids, Int. J. Heat Mass Transfer 49 (2006) 5070–5074.

[11] S.S. Kutateladze, Boiling heat transfer, Int. J. Heat Mass Transfer 4 (1961) 31–45.

[12] L.H. Lienhard, V.K. Dhir, Hydrodynamic predictions of peak pool-boiling heat flux from finite bodies, ASME J. Heat Transfer 95 (1973) 152–158.

[13] M. Maracy, R.H.S. Winterton, Hysteresis and contact angle effects in transition pool-boiling of water, Int. J. Heat Mass Transfer 31 (1988) 1443–1449.

[14] D. Milanova, R. Kumar, Role of ions in pool-boiling heat transfer of pure and silica nanofluids, Appl. Phys. Lett. 87 (2005) 233107.

[15] K. Sefiane, On the role of structural disjoining pressure and contact line pinning in critical heat flux enhancement during boiling of nanofluids, Appl. Phys. Lett. 89 (2006) 044106.

[16] G. Sethumadhavan, A. Nikolov, D.T. Wasan, Stability of liquid films containing monodisperse colloidal particles, J. Colloid Interf. Sci. 240 (2001) 105–112.

[17] A. Trokhymchuk, D. Henderson, A. Nikolov, D.T. Wasan, A simple calculation of structural and depletion forces for fluids/suspensions confined in a film, Langmuir 17 (2001) 4940–4947.

[18] S. Vafaei, T. Borca-Tascius, M.Z. Podowski, A. Purkayastha, G. Ramanath, P.M. Ajayan, Effect of nanoparticles on sessile droplet contact angle, Nanotechnology 17 (2006) 2523–2527.

[19] P. Vassallo, R. Kumar, S. Damico, Pool-boiling heat transfer experiments in silica–water nanofluids, Int. J. Heat Mass Transfer 47 (2004) 407–411.

[20] D.T. Wasan, A.D. Nikolov, Spreading of nanofluids on solids, Nature 423 (2003) 156–159.

[21] V.M. Wasekar, R.M. Manglik, Pool-boiling heat transfer in aqueous solutions of an anionic surfactant, ASME J. Heat Transfer 122 (2000) 708–715.

[22] P.C. Wayner, Intermolecular forces in change of phase heat transfer: 1998 Donald Q. Kern award review, AIChE J. 45 (1999) 2055–2068.

[23] D.S. Wen, Y.L. Ding, R. Williams, Thermal nanofluids for heat intensification applications, Chem. Eng. 771 (2005) 32–34.

[24] D.S. Wen, Y.L. Ding, Experimental investigation into the pool-boiling heat transfer of aqueous based – Al_2O_3 nanofluids, J. Nanoparticle Res. 7 (2005) 265–274.

[25] D.S. Wen, Y.L. Ding, R. Williams, Pool-boiling heat transfer of aqueous based TiO_2 nanofluids, J. Enhanced Heat Transfer 13 (2006) 231–244.

[26] D.S. Wen, B.X. Wang, Effects of surface wettability on nucleate pool-boiling heat transfer for surfactant solutions, Int. J. Heat Mass Transfer 45 (2002) 1739–1747.

[27] S.M. You, J.H. Kim, K.H. Kim, Effect of nanoparticles on critical heat flux of water in pool-boiling heat transfer, Appl. Phys. Lett. 83 (2003) 3374–3376.

[28] S.J. Haa, H.C. No, A dry-spot model of critical heat flux applicable to both pool-boiling and sub-cooled forced convection boiling, Int. J. Heat Mass Transfer 43 (2000) 241–250.

[29] T.G. Theofanous, T.N. Dinh, J.P. Tu, A.T. Dinh, The boiling crisis phenomenon Part II: dryout dynamics and burnout, Exp. Therm. Fluid Sci. 26 (2002) 793–810.

[30] Y.H. Zhao, T. Masuoka, T. Tsuruta, Unified theoretical prediction of fully developed nucleate boiling and critical heat flux based on a dynamic microlayer model, Int. J. Heat Mass Transfer 45 (2002) 3189–3197.

[31] N. Zuber, On stability of boiling heat transfer, ASME J. Heat Transfer 80 (1958) 711–720.